Connectivity Improvement in Wireless Sensor Networks Using ESPAR Antennas with Dielectric Overlays

Luiza Leszkowska*[1], Mateusz Rzymowski*[2], Marcin Madziąg[+], Krzysztof Nyka*[3], Łukasz Kulas*[4]

*Department of Microwave and Antenna Engineering, Gdansk University of Technology, Faculty of Electronics, Telecommunications and Informatics, Gdansk, Poland

[+]ISS RFID sp. z o.o., Gdynia, Poland

{[1]luiza.leszkowska, [2]mateusz.rzymowski, [3]krzysztof.nyka, [4]lukasz.kulas}@pg.edu.pl, [+]marcin.madziag@issrfid.com

Abstract—**This article presents an electrically steerable parasitic array radiator (ESPAR) switched beam antenna with a dielectric overlay to miniaturize the antenna and modify the radiation pattern in the vertical plane. The antenna is intended for a gateway in a wireless sensor network (WSN) and is located on the ceiling of a room. Because the ESPAR antenna consists of an array of vertical monopoles, there is a deep minimum in the radiation pattern right beneath the antenna. The use of a dielectric overlay improves the radiation pattern in the vertical direction. Systematic tests in realistic indoor environment in the 2.4 GHz frequency band were conducted, which showed improved connectivity with wireless sensors placed near the floor in a wide area beneath the antenna.**

Keywords— switched-beam antenna, electronically steerable parasitic array radiator (ESPAR), wireless sensor network

I. INTRODUCTION

In smart farming applications, information acquired from Internet of Things (IoT) sensors will play pivotal role for better management of crops or livestock to influence overall productivity as well as more sustainable operations [1]. In many applications, IoT agricultural network architecture relies on Wireless Sensor Network (WSN) nodes, which can be deployed for sensing, localizing, monitoring or actuating. In such IoT systems, dedicated WSN gateways, usually connected to and IP network, are used to provide reliable communication to WSN nodes.

For wireless sensor networks operating in dense or challenging real-life environments (e.g. indoors, rural or industrial), antennas with electronically switched directional beams used in WSN gateways can improve bandwidth, throughput or network capacity [2]-[5]. By choosing the right directional radiation pattern to focus the antenna beam towards a specific direction, WSN gateways equipped with such antennas can communicate more efficiently with surrounding WSN nodes. In result, one can easily obtain better overall network performance than when WSN gateways with dipole or monopole antennas with omnidirectional radiation patterns are used.

One of the most promising types of antennas enabling electronical beam switching are electronically steerable parasitic array radiator (ESPAR) antennas [6]-[9]. The radiation pattern is shaped by changing values of load impedances connected to passive elements surrounding a centrally placed active antenna which is connected to a signal source. To apply this concept in WSN nodes and gateways in
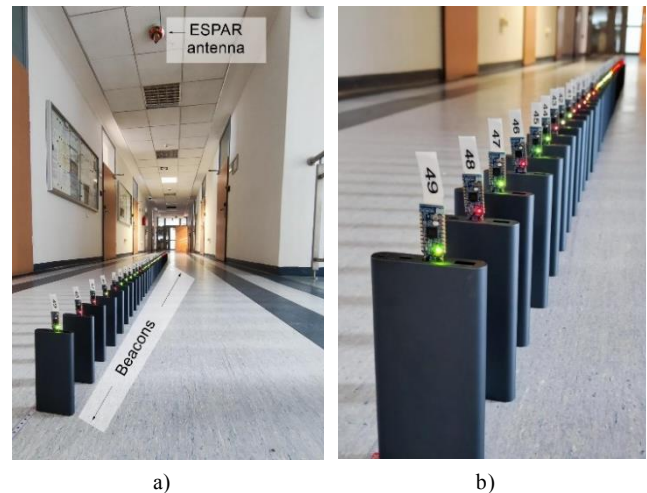

Fig. 1. Test setup arranged for the measurements: a) Test configuration overview; b) Beacons spaced at equal intervals of 10 cm.

a simple way, low-cost and low-current integrated single-pole double-throw (SPDT) FET switches were proposed to provide electronically switchable load impedances close to an open or short circuit at each of 12 passive elements ends [7]-[9]. In result, 12 directional radiation patterns are available in WSN nodes or gateways, in which simple and inexpensive transceivers are integrated with such ESPAR antennas [8].

One of the main drawbacks of a standard ESPAR antenna is a blind spot along the axis of the radiating monopole. When an ESPAR antenna is integrated within WSN gateways mounted indoors at the ceiling, this blind spot will appear directly under the antenna and it will deteriorate connectivity parameters to WSN nodes placed underneath. One of the possible ways to mitigate this effect is to use ESPAR antenna embedded within a dielectric overlay, which was originally used to miniaturize the antenna [10],[11]. Further investigations of 3D printed dielectric overlays influence on ESPAR antenna parameters revealed that the use of such overlay affects also ESPAR antenna radiation patterns in elevation plane [12],[13] increasing radiating power directly beneath the antenna. However, according to the authors best knowledge, systematic measurements have not been yet reported.

In this article, we demonstrate how the use of a 3D printed dielectric overlay that improves the radiation pattern in the vertical direction affects connectivity in the 2.4 GHz frequency band between an ESPAR equipped WSN gateway

mounted at the ceiling and WSN nodes placed underneath. To this end, we present results of systematic tests, in which 50 beacons (WSN nodes) were used in a realistic indoor environment to simultaneously sample the distribution of

received signal strength. The results show improved connectivity with wireless sensors placed near the floor in a wide area beneath the antenna.

II. ANTENNA DESIGN

A. ESPAR Antenna

The use of a switched-beam antenna such as ESPAR antenna presented in Fig. 2 can be an effective way of ensuring efficient communication in indoor applications. The antenna used to conduct tests in this study was designed for the 2.4 GHz frequency band. It employs electrical switching based on integrated FET switches NJG1681 to reconfigure the radiation pattern. The antenna consists of a circular ground plane, single active monopole and 12 passive elements which are connected to the SPDT switches for alternating their function between director and reflector. To form an optimally shaped directive beam, the passive 5 adjacent elements work as the directors while the other ones are the reflectors. By rotating this setup sequentially, antenna allows for full rotation of the beam in the horizontal plane. The maximum radiation of the directional beam in the elevation plane is at 60 degrees relative to the central axis of the antenna. The half power beamwidth (HPBW) covers the angular range from 34 to 98 degrees, which means that communication with devices located under the antenna may be ineffective.

B. ESPAR Antenna with 3D Printed Overlay

The antenna shown in Fig. 3 is a modified version of standard ESPAR antenna which has an dielectric overlay added to embed all the monopoles. This enhancement, besides the reduction of the antenna size, reshapes the beam in such a way that it reaches the angles unavailable for the standard ESPAR antenna. HPBW covers the angular range up to 2 degrees below the antenna while the maximum of the radiation pattern is at 50 degrees relative to antenna axis. The dielectric overlay is a cylinder of diameter 64.8 mm and height 24.4 mm placed on the antenna ground plane and fabricated in 3D printing process using PLA filament with permittivity equal to 2.62, loss tangent 0.005 determined by measuring samples printed with the same printer settings.

III. TEST SETUP

A. Reference Test Setup for Standard ESPAR Antenna

The presented reference test setup utilizes a reconfigurable ESPAR antenna with 12 passive elements able to generate 12 directional beams called C_i (for $i = 1, \ldots 12$) and 2 omnidirectional beams. The antenna was mounted on the ceiling and 49 beacons (signaling devices) were placed along a straight line under the antenna Each beacon is dedicated unit including an nRF52840 SoC with an integrated antenna for low-energy wireless communication in Bluetooth LE standard. The purpose of this setup is to investigate the communication efficiency to verify the blind spot effect at short distances measured from the point directly under the
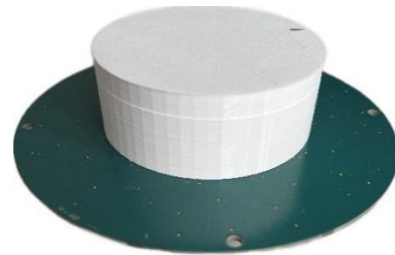

Fig. 2. ESPAR antenna.

Fig. 3. ESPAR antenna with 3D printed overlay.

antenna. Therefore the beacons were distributed along a corridor in an office building at a total distance up to 2.4 m in two directions as shown in Fig. 1. The corridors opens to a staircase at the side corresponding to distances marked as positive values while the other side has negative values of a coordinate. The space between beacons was constant and equal 10 cm. Each beacon transmitted packets of 31 bytes with time interval of 250 ms. The power of the beacons was set to 8 dBm. The communication was examined for two orientations of the beacons' antennas – parallel and perpendicular to the line on which they were placed. The parallel orientation is expected to provide better polarization alignment between the ESPAR and the beacons.

B. Test Setup for ESPAR Antenna with Dielectric Overlay

As mentioned in Section II A, in the case of the base ESPAR antenna, there is an area of impaired communication under the antenna. To mitigate this problem, an ESPAR antenna with a dielectric overlay presented Section II B has been proposed. Although the dielectric overlay has already been reported as mean to reduce the antenna size, the ESPAR antenna used in this experiment has been designed mostly to connectivity by reshaping the beam. The connectivity tests for the antenna with overlay were conducted in the same test setup and configurations as for the reference measurements presented in Section III A.

IV. RESULTS

A. RSSI level

The level the Received Signal Strength Indication (RSSI) was measured and averaged for all received packets. All tests were carried out using all 12 directional beams ($C1 - C12$) and 2 omnidirectional beams possible to obtain in the antenna and for two beacon alignments: situation (A), in which the beacons are placed parallel to each other as shown in Fig. 1, and
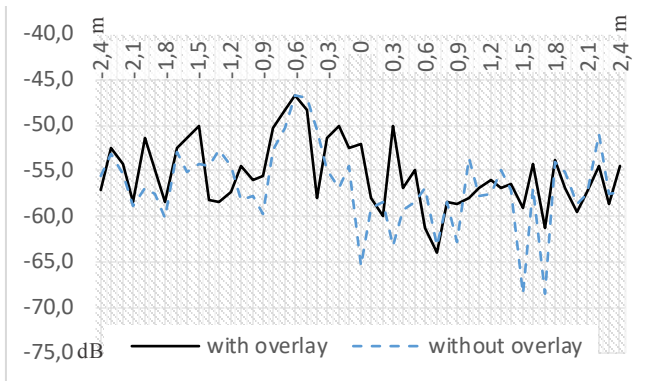
169

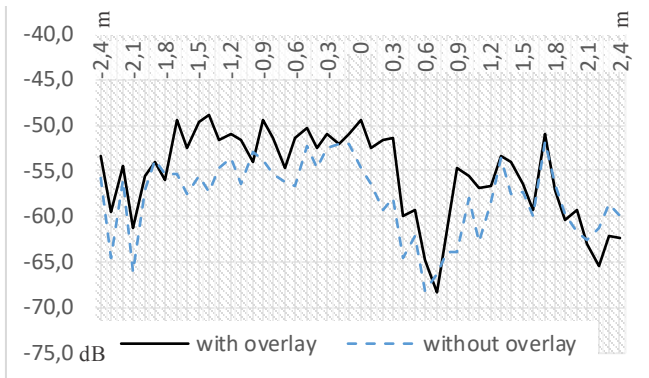Fig. 4. Average RSSI (averaged values for beams C5 and C11) – beacons placed in parallel (A).

Fig. 6. RSSI (beam C5 and C11 for negative and positive coordinates respectively) – beacons placed in parallel (A).

Fig. 5. Average RSSI (averaged values for beams C5 and C11) – beacons in position rotated by 90 degrees (B).

Fig. 7. RSSI (beam C5 and C11 for negative and positive coordinates respectively) – beacons in position rotated by 90 degrees (B).

situation (B), in which the beacons were rotated by 90 degrees relative to the situation (A). Theses settings correspond to the orthogonal and parallel orientation of the beacons' antennas. The results are presented with respect to variable distance of the beacons from the point under the gateway antenna, for the standard ESPAR antenna (blue dashed line) and ESPAR antenna with an overlay (solid black line). The distance is represented by a positive or negative coordinate value in meters. Fig. 4 presents the level of RSSI in situation (A) which was additionally averaged for different configurations of the antenna beam. The antenna configurations were limited to two directional beams: C5 antenna configuration having maximum radiation towards beacons with negative coordinates and C11 antenna configuration having maximum radiation towards beacons with positive coordinates. Similarly, Fig. 5 shows corresponding results for situation (B). In both cases, some smoothing of the deep minima of the characteristics can be observed as an effect of using the antenna with overlay except for the strong minimum in situation (B) occurring around 0.6 m, which was probably caused by reflections from a metal bar barrier near the staircase and stronger two-path effects due to reflection form the floor. This effect is even more visible when taking under consideration only the beams in the directions towards the beacons, which is beam C5 and C11 for negative and positive coordinates respectively (Fig. 7). For the same beam configuration and the
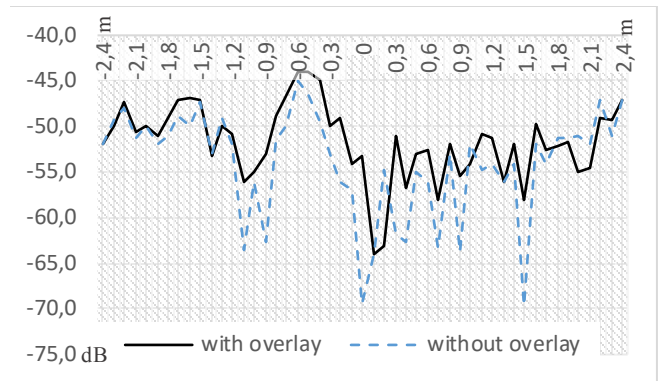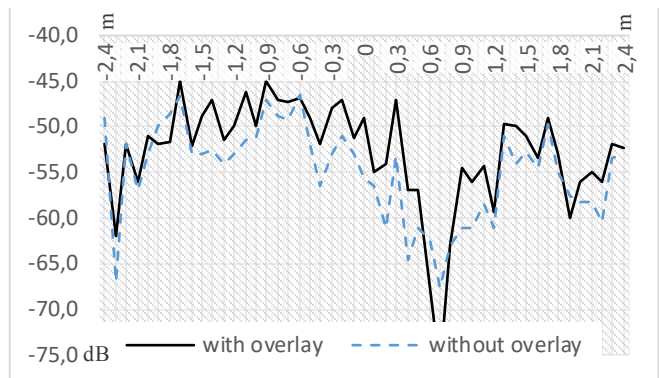
situation (A), there is a deep minimum directly under the ESPAR antenna, which is significantly improved by using the antenna with overlay, as seen in Fig. 6. For all the measurement configurations the antenna with overlay performs better with respect to RSSI, especially for shorter distances, however, for the configuration (B), the improvement is slightly stronger. Table I shows the RSSI values measured directly under the reconfigurable antenna in configurations C5 and C11 considered separately, as well as the averaged values from the distance range from 0 to 0.5 m, 1 m and 1.5 m in both directions for configurations C5 or C11 chosen depending of the position of the beacons (pointing towards a beacon). In Table I, there is also the average RSSI for the entire range of measurement distances and all 14 antenna beam configurations. In each case, the RSSI values for the ESPAR antenna with overlay are higher than for the standard ESPAR antenna.

B. Packet Delivery Ratio

The packet delivery ratio (PDR), which is the ratio of the number of received packets to the number of sent packets, was also examined for the same measurement configurations. The results presented in Fig. 8, Fig. 9 and summarized in Table II show an improvement due to the usage of the antenna with overlay, however, the best improvement occurs for the situation (A). These results are consistent with the results for RSSI.

170

TABLE I.   Comparison of RSSI Level

RSSI level [dB]	Test scenario			
	Without overlay (A)	With overlay (A)	Without overlay (B)	With overlay (B)
Distance 0 m (*C5 configuration*)	-69.5	-53.2	-55.6	-49.0
Distance 0 m (*C11 configuration*)	-61.5	-51.0	-54.0	-50.0
Distance range 0 to 0.5 m (*averaged for C5 and C11*)	-57.2	-53.0	-56.1	-51.5
Distance range 0 to 1 m (*averaged for C5 and C11*)	-56.3	-52.5	-56.0	-53.3
Distance range 0 to 1.5 m (*averaged for C5 and C11*)	56.0	-52.5	-55.4	-52.5
Distance range 0 to 2.4 m (*averaged for C5 and C11*)	-54.0	-51.7	-55.0	-52.8
Distance range 0 to 2.4 m (*all configurations*)	-56.6	-55.4	-57.1	-55.8

TABLE II.   Comparison of Packet Delivery Ratio

Packets / PDR	Test scenario			
	Without overlay (A)	With overlay (A)	Without overlay (B)	With overlay (B)
Packets received (*all configurations*)	1979	2173	2394	2464
Packet sent (*all configurations*)	4014	3819	3844	4009
PDR (*all configurations*)	49.3%	56.9%	62.3%	61.5%
PDR (*averaged for C5 and C11*)	81.0%	84.2%	85.5%	87.9%
PDR (*C5 or C11 used to direct beam towards beacons*)	77.9%	84.2%	87.4%	87.6%

direction. The measurement results show that with respect to RSSI and PDR, the antenna with overlay outperforms the standard ESPAR antenna. Although the improvement is not significant, it is obtained at no additional cost, because the primary goal for the dielectric overlay is to reduce the antenna size.
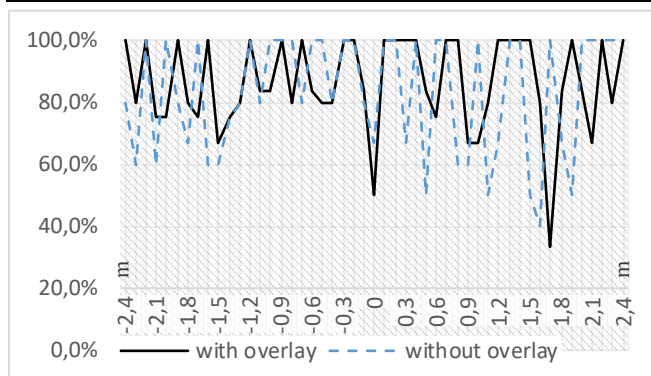

Fig. 8. Packet delivery ratio (beam C5 and C11 for negative and positive coordinates respectively) – beacons placed in parallel (A).
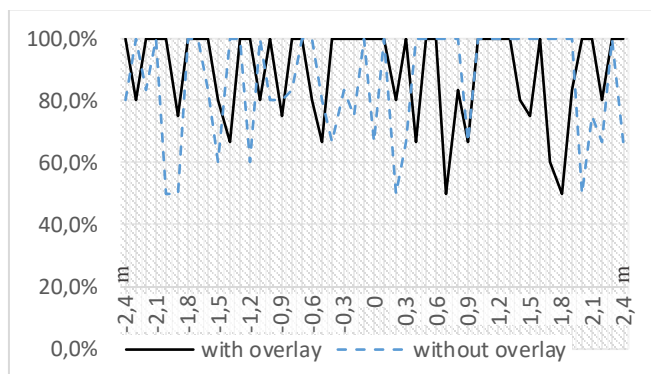

Fig. 9. Packet delivery ratio (beam C5 and C11 for negative and positive coordinates respectively) – beacons in position rotated by 90 degrees (B).

V. Conclusions

The connectivity performance for indoor communication in Bluetooth LE standard was experimentally investigated for two switched beam ESPAR antenna types used in a WSN gateway mounted on the ceiling in an office building. The results for RSSI and PDR were compared for a standard 12-element ESPAR antenna and a similar antenna with a dielectric overlay added to reduce the antenna size. To achieve an additional effect of connectivity improvement, the antenna with the overlay was design to have its beam in more vertical

References

[1] M. S. Farooq, S. Riaz, A. Abid, K. Abid and M. A. Naeem, "A Survey on the Role of IoT in Agriculture for the Implementation of Smart Farming," in IEEE Access, vol. 7, pp. 156237-156271, 2019, doi: 10.1109/ACCESS.2019.2949703

[2] J. N. Al-Karaki and A. Gawanmeh, "The Optimal Deployment, Coverage, and Connectivity Problems in Wireless Sensor Networks: Revisited," in IEEE Access, vol. 5, pp. 18051-18065, 2017.doi: 10.1109/ACCESS.2017.2740382

[3] T. Tran, M. K. An, D. T. Huynh, "Symmetric connectivity in wsns equipped with multiple directional antennas", Proc. Int. Conf. Comput. Netw. Commun. (ICNC), pp. 609-614, Jan. 2017.

[4] L. Catarinucci, S. Guglielmi, R. Colella and L. Tarricone, "Compact Switched-Beam Antennas Enabling Novel Power-Efficient Wireless Sensor Networks," in IEEE Sensors Journal, vol. 14, no. 9, pp. 3252-3259, Sept. 2014. doi: 10.1109/JSEN.2014.2326971

[5] F. Ademaj, M. Rzymowski, H. -P. Bernhard, K. Nyka and L. Kulas, "Relay-Aided Wireless Sensor Network Discovery Algorithm for Dense Industrial IoT Utilizing ESPAR Antennas," in IEEE Internet of Things Journal, vol. 8, no. 22, pp. 16653-16665, 15 Nov.15, 2021

171

[6] E. Taillefer, A. Hirata, and T. Ohira, "Direction-of-arrival estimation using radiation power pattern with an ESPAR antenna," IEEE Trans. Antennas Propag., vol. 53, no. 2, pp. 678–684, Feb. 2005.

[7] L. Kulas, " RSS-based DoA Estimation Using ESPAR Antennas and Interpolated Radiation Patterns," IEEE Antennas Wireless Propag. Lett., vol. 17, no. 1, pp. 25-28, Jan. 2018.

[8] M. Groth, M. Rzymowski, K. Nyka and L. Kulas, "ESPAR Antenna-Based WSN Node With DoA Estimation Capability," in IEEE Access, vol. 8, pp. 91435-91447, 2020, doi: 10.1109/ACCESS.2020.2994364.

[9] Groth, M.; Nyka, K.; Kulas, L. Calibration-Free Single-Anchor Indoor Localization Using an ESPAR Antenna. *Sensors* 2021, *21*, 3431.

[10] Junwei Lu, D. Ireland and R. Schlub, "Dielectric embedded ESPAR (DEESPAR) antenna array for wireless communications," IEEE Trans. Antennas Propag., vol. 53, no. 8, pp. 2437-2443, Aug. 2005.

[11] M. Czelen, M. Rzymowski, K. Nyka and L. Kulas, "Miniaturization of ESPAR Antenna Using Low-Cost 3D Printing Process," 2020 14th European Conference on Antennas and Propagation (EuCAP), Copenhagen, Denmark, 2020, pp. 1-4.

[12] M. Czelen, M. Rzymowski, K. Nyka and L. Kulas, "Influence of Dielectric Overlay Permittivity on Size and Performance of Miniaturized ESPAR Antenna," 2020 23rd International Microwave and Radar Conference (MIKON), Warsaw, Poland, 2020, pp. 289-292.

[13] M. Czelen, M. Rzymowski, K. Nyka and L. Kulas, "Influence of Dielectric Overlay Dimensions on Performance of Miniaturized ESPAR Antenna," 2020 IEEE International Symposium on Antennas and Propagation and North American Radio Science Meeting, Montreal, QC, Canada, 2020, pp. 387-388.

172